J. Phys. Chem. A **2009,** *113,* 3545–3554

Effect of Halogenation on the Mechanism of the Atmospheric Reactions between Methylperoxy Radicals and NO. A computational Study

Agnie M. Kosmas,*,[†] Zoi Salta,[†] and Antonija Lesar[‡]

Division of Physical Chemistry, Department of Chemistry, University of Ioannina, Greece 45110, and Department of Physical and Organic Chemistry, Insitute Jožef Stefan, Jamova c.39, SI-1000, Ljubljana, Slovenia

Received: March 12, 2008; Revised Manuscript Received: February 17, 2009

The mechanism of the reactions between the halogenated methylperoxy radicals, CHX_2O_2 (X = F, Cl), and NO is investigated by using ab initio and density functional quantum mechanical methods. Comparison is made with the mechanism of the CH_3O_2 + NO reaction. The most important energy minima in the potential energy surface are found to be the two conformers of the halogenated methyl peroxynitrite association adducts, CHX_2OONOcp and CHX_2OONOtp, and the halogenated methyl nitrates, CHX_2ONO_2. The latter are suggested to be formed through the one-step isomerization of the peroxynitrite adduct and may lead upon decomposition to carbonylated species, CX_2O + HONO and CHXO + XNO_2. The ambiguous issue of the unimolecular peroxynitrite to nitrate isomerization is reconsidered, and the possibility of a triplet transition state involvement in the ROONOtp ↔ $RONO_2$ rearrangement is examined. The overall calculations and the detailed correlation with the methyl system show the significant effect of the halogenation on the lowering of the entrance potential energy well which corresponds to the formation of the peroxynitrites. The increased attractive character of the potential energy surface found upon halogenation combined with the increased exothermicity of the CHX_2O_2 + NO → CHX_2O + NO_2 reaction are suggested to be the important factors contributing to the enhanced reactivity of the halogenated reactions relative to CH_3O_2 + NO. The calculated heat of formation values indicate the large stabilization of the fluorinated derivatives.

Introduction

Alkylperoxy radicals are produced in the degradation process of hydrocarbons in the troposphere.[1] In regions with high concentrations of NO, they form energized peroxynitrite molecules which decompose to alkoxy radicals and NO_2.[2,3]

$$RO_2 + NO \rightarrow ROONO \rightarrow RO + NO_2 \qquad (1a)$$

The secondary channel, leading to the formation of alkyl nitrates,[4] has been also extensively discussed.

$$RO_2 + NO \rightarrow RONO_2 \qquad (1b)$$

Because of the importance of reaction 1 in atmospheric chemistry, numerous experimental investigations of the kinetics of these systems have been reported, several of them being devoted to the reactions of the halogenated radicals.[5−19] These studies suggest that halogenation generally promotes the reactivity of C_1 haloalkylperoxy radicals toward NO.[8] For instance, the rate coefficient of the reaction CF_3O_2 + NO, 1.6×10^{-11} $cm^3\ mol^{-1}\ s^{-1}$ at room temperature,[20] is larger than that of CH_3O_2 + NO, 7.7×10^{-12} $cm^3\ mol^{-1}\ s^{-1}$.[20,21] The $CHClO_2$ + NO and $CHBr_2O_2$ + NO reactions also present larger rate constants, 1.9×10^{-11} and 1.1×10^{-11} $cm^3\ mol^{-1}\ s^{-1}$, respectively, at 298 K.[20] The enhancement of the rate coefficient has been attributed to a possible reduction of the peroxide RO—O bond strength in the intermediate peroxynitrite association minimum, because of the halogen electron withdrawing effect.[8] An analogous inductive effect may be invoked for the larger rate constant of the reaction $CH_3C(O)O_2$ + NO, $(2.1 \pm 0.5) \times 10^{-11}$ $cm^3\ mol^{-1}\ s^{-1}$ at 313 K.[22]

Parallel to the experimental studies, several theoretical investigations have been reported.[23−31] King and Thomson[23] have examined the reactivity of RO_2 radicals toward NO in terms of the difference of SOMO (singly occupied MO) energies between the two reactants and found that chloroalkylperoxy radicals present more negative E_{SOMO} values than those with methyl substituents, justifying the higher reactivity of the former toward NO. Several other theoretical investigations focused primarily on the simplest system, the reaction CH_3O_2 + NO.[24−31] The modeling of the potential energy surface (PES) has established the intermediate formation of both cis and trans conformers of the nascent association methyl peroxynitrite adduct.[24−28] The two conformers differ only byaround 1−2 kcal mol^{-1} in stability by all computational methods employed, and thus, they are formed with a nearly equal probability.[24−28] The cis conformer dissociates directly to radical pair formation, CH_3O + NO_2, whereas the trans structure was suggested to isomerize to CH_3ONO_2.[28] The latter can further dissociate to CH_3O + NO_2 or thermalize under suitable atmospheric conditions. However, the isomerization transition state [ROONOtp ↔ $RONO_2$] (R = CH_3 and R= H for the analogous hydroperoxy system as well) determined at the B3LYP level of theory has been much criticized.[29] Arenas et al,[30] by using multiconfigurational perturbation theory techniques, showed that no such isomerization transition state exists on the singlet surface. They suggested instead a two-step mechanism according to which CH_3ONO_2 is formed as the recombination energy minimum in

---

* Corresponding author.

[†] University of Ioannina.

[‡] Insitute Jožef Stefan.

10.1021/jp808895a CCC: $40.75

the reverse reaction between the alkoxy radical, CH_3O and NO_2, produced from the dissociation of the energized methyl peroxynitrite

$$CH_3O_2 + NO \leftrightarrow CH_3OONO \leftrightarrow CH_3O + NO_2 \leftrightarrow CH_3ONO_2 \quad (2)$$

Such a two-step mechanism is quite unlikely and can only operate in the very low pressure regime if the radical pair forms a weak complex. As a rule, the methoxy radical, CH_3O, produced under moderate pressure or atmospheric conditions, will be vibrationally excited and will most frequently decompose. If not, it will react with the much more abundant O_2 rather than with NO_2. Hence, the two-step pathway is highly improbable, and the question about a proper mechanism governing alkyl nirate production under a more realistic range of pressures[32,33] still remains unanswered.

In view of the numerous experimental reports involving halogenated peroxy radicals, the computational investigation of the halogenation effect would also be desirable. Yet, theoretical reports on halogenated systems, to the best of our knowledge, have been quite scarce. McGivern et al.[34,35] have examined several energy features of the brominated systems, NO + CH_2BrO_2, $CHBr_2O_2$, and CBr_3O_2, as part of the investigation of the atmospheric oxidation pathways of brominated methanes. Also Lesar et al.[36,37] have recently studied the structural and thermodynamic properties of a series of chlorinated and fluorinated methyl peroxynitrites and nitrates. The interesting feature emerging from these limited studies is the increased stabilization of the intermediate alkyl peroxynitrite relevant to the alkylperoxy radical + NO reactants upon halogenation. Detailed comparison of these results with the plain methyl system[27,28] to the degree allowed by the similarity of the methods employed shows a larger stabilization energy of the intermediate halogenated methyl peroxynitrites with respect to CXH_2O_2 + NO in comparison with CH_3OONO versus CH_3O_2+NO. As a result, the reactions CXH_2O_2 + NO present a steeper slope and a deeper potential well in the entrance valley of the PES. Hence, the enhancement of the rate coefficient and the increased reactivity of the halogenated reactions must originate from the differentiation of the PES relative to the CH_3O_2 + NO surface rather than be attributed to a weakening of the halogenated peroxy bond as initially assumed. In fact, Lesar et al.,[36] in the examination of the structural features of quite a number of halogenated methyl peroxynitrites, have shown that halogenation brings no change to the peroxy bond distance in the intermediate peroxynitrites and no weakening of the peroxy bond. Instead, the main structural changes observed were the significant reduction of the C—OO bond and the severe elongation of the OO—N bond, whereas the peroxide bond distance remains entirely unaffected by the introduction of halogen atoms in the methylic group.

Motivated by these findings, we have undertaken in the present work the investigation of the main energy minima and critical energy barriers of the reactions CHX_2O_2 + NO (X = F, Cl) and the analysis of the most important changes in the PES brought about by the halogen induction effect. A good portion of the work is devoted to the reconsideration of the peroxynitrite to nitrate one-step rearrangement, $CH_3OONO \leftrightarrow CH_3ONO_2$, and the reformulation of a plausible mechanism for this process, which could serve as the model for the halogenated systems and the corresponding $CHX_2OONO \leftrightarrow CHX_2ONO_2$ conversions as well.

Computational Details

Geometry optimizations and vibrational harmonic frequency analysis have been performed by using ab initio and density functional theory techniques, namely, the second-order unrestricted Møller—Plesset perturbation theory (U)MP2[38,39] and the (U)B3LYP[40,41] functional, combined with the 6—-1G(d) and the 6-311++G(d,p) basis sets.[42] Minima and transition states were characterized by the harmonic vibrational frequency analysis. Intrinsic reaction coordinate[43] calculations were used to follow the reaction path and confirm its course in both directions from the transition states to the corresponding reactants and products. Anharmonic frequencies of the stable adducts were evaluated at the more economical B3LYP level, and the energetics were further refined by employing G2(MP2), G3//B3LYP, and single-point CCSD(T)/6-311++G(d,p) calculations[44] based on the MP2 and B3LYP optimized geometries.

In order to explore a plausible mechanism for the one-step $CH_3OONO \leftrightarrow CH_3ONO_2$, $CHX_2OONO \leftrightarrow CHX_2ONO_2$ isomerizations, a point-by-point exploration of the conversion process on both the singlet and the triplet states has been carried out at the (U)B3LYP/6-311++G(d,p) theory level. The computation produced interesting and suggestive ideas regarding the detailed mechanism of the unimolecular rearrangement process.

The heat of formation values, ΔH_f for the important energy minima, that is, the halomethylperoxy nitrites and the halomethyl nitrates, were determined by using G2(MP2), G3//B3LYP, and CBS-Q//B3LYP computational thermochemistry protocol[45] by following the procedure based on atomization energies, as outlined by Curtiss et al.[46] A second and third series of ΔH_f values have also been calculated on the basis of the dissociation processes calculated in the present work

$$CHX_2OONO \rightarrow CHX_2O + NO_2 \quad (3a)$$

$$CHX_2ONO_2 \rightarrow CHX_2O + NO_2 \quad (3b)$$

and the use of the following isodesmic reaction at the G2MP2 level of theory

$$CH_2X_2 + CH_3ONO_2 \rightarrow CH_4 + CHX_2ONO_2 \quad (4)$$

The results from all procedures are summarized and compared in Table 3, where the excellent agreement between the CBS-QB3 heat of formation value for CH_3ONO_2 and the most recently tabulated value[20] gives a measure of the reliability of the computations.

All calculations have been carried out with the use of the Gaussian 03 series of programs.[47]

Results and Discussion

Table 1 summarizes selected structural data, and Figures 1 and 2 present the optimized structures of the most important energy minima and transition states determined in the investigation of the reactions CHX_2O_2 + NO (X = F, Cl). Figures 3 and 4 display the reaction energy profiles, and Figure 5 depicts the much discussed isomerization pathway profile in the maternal CH_3O_2 + NO system, that is, the methyl peroxynitrite to methyl nitrate conversion on the singlet and the triplet states. The energetics results are summarized in Table 2 where detailed comparison is made with the CH_3O_2 + NO reported values.[28] Relevant data about the $CHBr_2O_2$ + NO system taken from the

TABLE 1: Comparison of Selective Bond Distances (Å) in Important Energy Minima of the Reactions CHX_2O_2 + NO (X = H[a], F, Cl) by Using the 6-311++G(d,p) Basis Set

	C−O		CO-O		O−N		ON-O	
	MP2	B3LY	MP2	B3LYP	MP2	B3LYP	MP2	B3LYP
$CH_3OONOcp$	1.424	1.431	1.420	1.430	1.526	1.472	1.160	1.159
$CH_3OONOtp$	1.422	1.429	1.426	1.425	1.479	1.480	1.169	1.161
CH_3ONO_2	1.432	1.440			1.412	1.422	1.206	1.198
$CHF_2OONOcp$	1.378	1.381	1.423	1.427	1.626	1.509	1.145	1.149
$CHF_2OONOtp$	1.377	1.381	1.425	1.425	1.576	1.536	1.151	1.148
CHF_2ONO_2	1.396	1.403			1.470	1.474	1.195	1.186
$CHCl_2OONOcp$	1.388	1.381	1.420	1.426	1.630	1.510	1.144	1.149
$CHCl_2OONOtp$	1.386	1.381	1.423	1.423	1.579	1.543	1.151	1.147
$CHCl_2ONO_2$	1.399	1.395			1.487	1.497	1.192	1.185

[a] From ref 28.

work of McGivern et al.[34,35] are also included. Finally, Table 3 lists the calculated heat of formation values.

Stationary Points and Products in the PES of the Reaction CH_3O_2 + NO → CH_3O + NO_2. The structural features of the optimized geometries for the energy minima, transition states, and products (Table 1 and Supporting Information) when compared to the corresponding methyl species[28] demonstrate the influence of the increased size and the electron withdrawing effect upon substitution of methylic hydrogens by halogen atoms. For the halogenated methyl peroxynitrites and the methyl nitrates in particular, the most significant changes involve the significant shortening of the C—O and ON—O bonds and the considerable elongation of the O—NO bond relative to CH_3OONO and CH_3ONO_2.[36,37] It is interesting to note that the peroxy bond distance O—O remains practically constant regardless of the changes in the methyl group. Therefore, halogenation of the methyl fragment modifies the C—O, O—N, and N—O geometrical parameters of CHX_2OONO, CHX_2ONO_2 (X = F, Cl) adducts but leaves the peroxy bond distance unaffected. The conclusion is supported by the examination of the reported $CHBr_2OONO$ data[34] which follow exactly the same trends and present a peroxy bond length similar to that of the chlorinated and the fluorinated analogues. Consequently, the structural trends contradict the assumption originally made, namely, that the enhancement of the rate coefficient of the reactions of the halogenated methylperoxy radicals with NO results from the weakening of the peroxide bond.[8]

Consideration of the energetics of the halogenated systems presents particular interest and has direct consequences on the reaction mechanism. The two association peroxy nitrite conformers are formed barrierlessly in the entrance valley, and their relative stability with respect to each other remains unaltered upon halogenation; that is, the trans conformer is predicted to be around 1.5 kcal mol^{-1} or less higher than the cis structure in all cases. In contrast to the maternal system, the halogenated peroxy nitrites are located significantly lower relative to CHX_2O_2 + NO, compared with the plain methyl peroxynitrite conformers relative to CH_3O_2 + NO. Specifically, the dissociation energy $CHX_2OONOcp$ → CHX_2O_2 + NO increases by 5.1, 4.7, and 6.5 kcal mol^{-1} for X = F, Cl, and Br, respectively, at the CCSD(T)//MP2 level, compared to the dissociation energy $CH_3OONOcp$ → CH_3O_2 + NO. Analogous trends are obtained from the other theory levels employed which predict a similar increase of the dissociation energies, namely, 5.6 and 4.5 kcal mol^{-1} at the CCSD(T)//B3LYP level, 4.1 and 4.3 kcal mol^{-1} at the G2MP2 level, and 4.7 and 4.4 kcal mol^{-1} at the G3//B3LYP level for =F and Cl, respectively. No specific halogen effect is evident; that is, all halogenated species are additionally stabilized compared to CH_3OONO by an amount of energy ranging from 4 to 6 kcal mol^{-1} depending on the theoretical method employed and regardless of the kind of halogen involved. To summarize, halogenation increases the stabilization of CHX_2OONO relative to CHX_2O_2 + NO, compared to that of CH_3OONO relative to CH_3O_2 + NO, independently of the particular halogen atom present in the methyl fragment. Relevant is also the lowering of the conformational cis−trans isomerization transition state, TS*cp-tp*. Despite the larger volume of the halogenated methyl group, all methods employed predict a reduction of the isomerization barrier by 1−2 kcal mol^{-1} with respect to the cis conformer upon halogenation. Thus, the interconversion $CHX_2OONOcp$ ↔ $CHX_2OONOtp$ becomes more feasible than the corresponding $CH_3OONOcp$ ↔ $CH_3OONOtp$ process. The other important feature observed in the present calculations is the increased exothermicity of the reactions CHX_2O_2 + NO → CHX_2O + NO_2 compared to that of the reaction CH_3O_2 + NO → CH_3O + NO_2 (Figures 3 and 4), which may be considered to contribute to the larger reactivity of the halogenated systems. The critical energy (Table 2) for CHX_2O + NO_2 production decreases relative to the reactants CHX_2O_2 + NO, from −11.0 kcal mol^{-1} for X = H to −14.3, −16.0, and −17.4 kcal mol^{-1} for X = F, Cl, and Br respectively, at the CCSD(T)//MP2 level. Similar trends are followed by the results of the other theory levels and reconfirm that halogenation causes a considerable overall energy lowering of the CHX_2O_2 + NO → CHX_2OONO → CHX_2O + NO_2 process. The increased attractive character of the PES correlates well with the enhancement of the rate coefficient of the halogenated alkylperoxy radicals toward NO. This overall energy lowering due to the halogen induction effect, which leads to a deeper entrance potential energy well and a lower critical energy for the production of the radical pair CHX_2O + NO_2, is the critical factor that affects significantly the reactivity of the latter systems compared to the methyl one.

Opposite to the exothermicity trends of the overall CHX_2O_2 + NO → CHX_2O + NO_2 system, the critical energy for the CHX_2OONO → CHX_2O + NO_2 dissociation step appears insensitive to halogenation. The radical pair CHX_2O + NO_2 is located higher than $CHX_2OONOcp$ by more or less a similar amount for all X, namely, by 10.0, 11.8, 9.7, and 10.1 kcal mol^{-1} at the CCSD(T)//MP2 level for X = H, F, Cl, and Br, respectively. At the G3//B3LYP level, the corresponding values are comparable too, 12.2, 15.2, and 12.7 kcal mol^{-1} for X = H, F, and Cl, respectively. Only fluorination appears to induce a very mild effect, arising most probably from the particular stability of fluorinated methoxy radicals. The alkoxy radical and NO_2 may recombine to form halogenated methyl nitrates. Now, in contrast to the CHX_2O_2 + NO ↔ CHX_2OONO process, the stabilization energy of methyl nitrates relative to RO_2 + NO shows negligible dependence on halogenation, meaning that

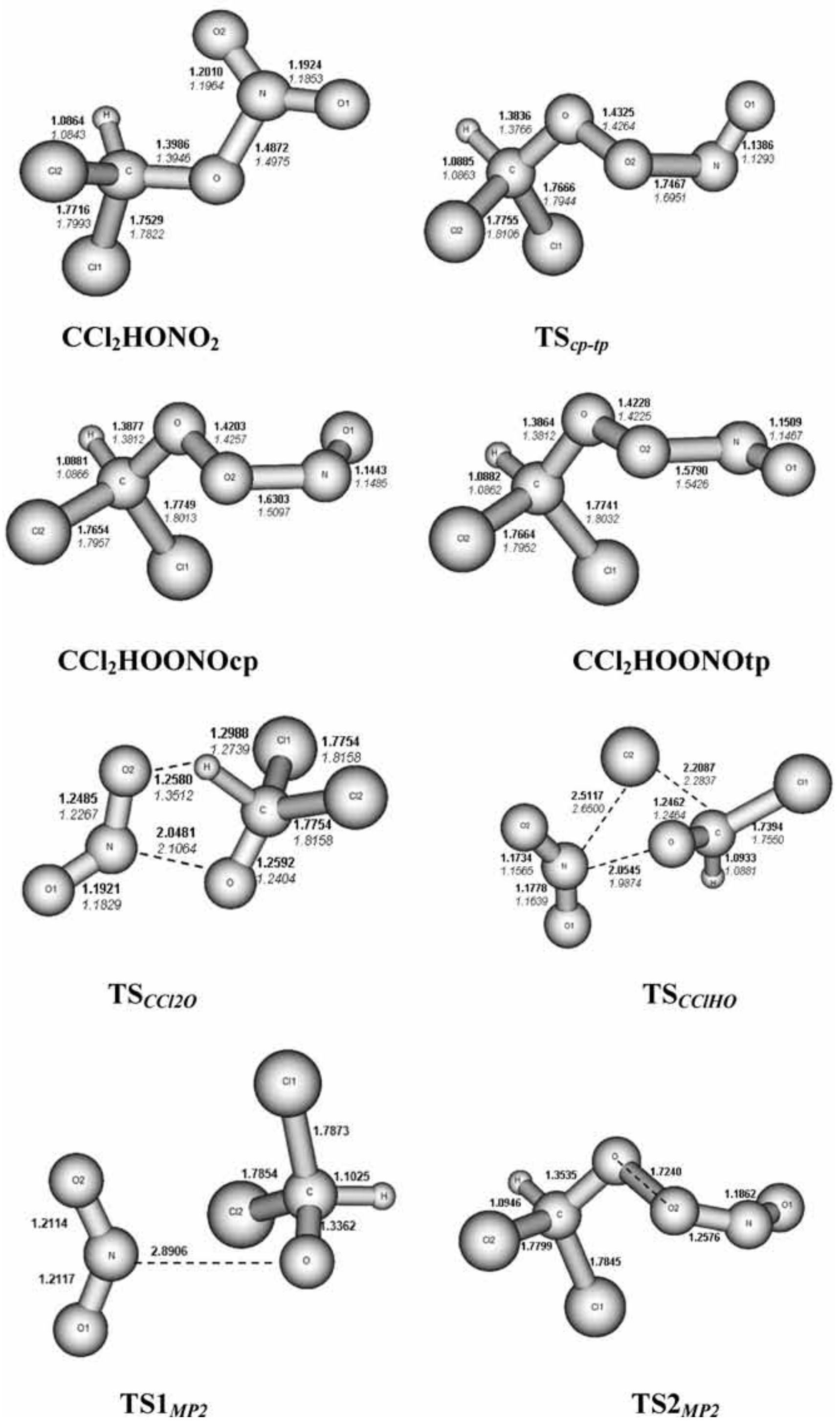

CCl_2HONO_2 $TS_{cp\text{-}tp}$

$CCl_2HOONOcp$ $CCl_2HOONOtp$

TS_{CCl2O} TS_{CClHO}

$TS1_{MP2}$ $TS2_{MP2}$

Figure 1. Optimized structures for the most important stationary points of the reaction $CHCl_2O_2$ + NO, at the MP2 (normal) and B3LYP (italics) levels of theory.

fluorination and chlorination of the methyl group does not affect the stability of CHF_2ONO_2 and $CHCl_2ONO_2$ relative to CHF_2O_2 + NO and $CHCl_2O_2$ + NO, respectively. The corresponding dissociation energies are 47.5, 47.1, and 47.5 kcal mol^{-1} at the CCSD(T)//MP2 level for X = H, F, and Cl, respectively, and similar by all other methods. However, stabilization of the halomethyl nitrates with respect to RO + NO_2 does exhibit a dependence on halogenation. The dissociation energies $CHX_2ONO_2 \rightarrow CHX_2O + NO_2$ present a decreasing trend, that is, 36.5, 32.8, and 31.5 kcal mol^{-1} for X = H, F, and Cl, respectively, at the CCSD(T)//MP2 level and 41.4, 39.0, and 36.2 kcal mol^{-1} at the G3//B3LYP level, showing in this way also a dependence on the halogen atom involved. In other words, the stabilization tendencies of methyl peroxynitrites and methyl nitrates follow quite different directions upon halogenation: halomethyl peroxynitrites are lowered in energy with respect to RO_2 +,NO, whereas halomethyl nitrates do not. Relative to the radical pair $CHX_2O + NO_2$, the stabilization of methyl peroxynitrites is little affected by halogenation, whereas that of alkyl nitrates, $CHX_2ONO_2 \rightarrow CHX_2O + NO_2$, is considerably influenced. Consequently, both reactions, that is, CHX_2O_2 + NO → $CHX_2OONO \rightarrow CHX_2O + NO_2$ and $CHX_2O + NO_2 \rightarrow CHX_2ONO_2$ → products are affected by halogenation, and the intermediate association minima in each case, CHX_2OONO and

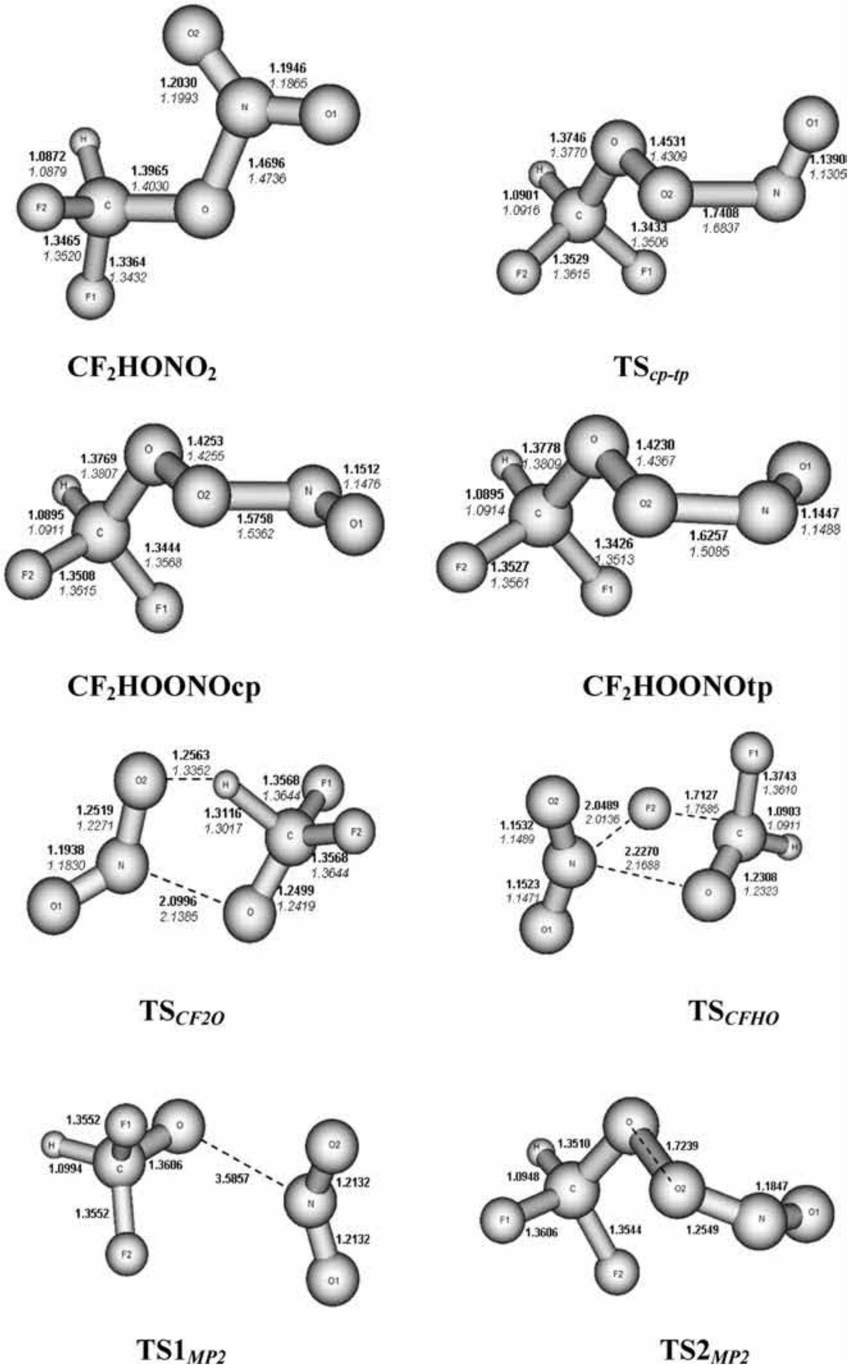

CF_2HONO_2 $TS_{cp\text{-}tp}$

$CF_2HOONOcp$ $CF_2HOONOtp$

TS_{CF2O} TS_{CFHO}

$TS1_{MP2}$ $TS2_{MP2}$

Figure 2. The same as in Figure 1 for the reaction CHF_2O_2 + NO.

CHX_2ONO_2, respectively, appear to play no role in the mechanism of the other reaction. It is also of interest to note the influence of halogenation in the relative energy between methyl peroxynitrite and methyl nitrate. CH_3ONO_2 is more stable than $CH_3OONOcp$ by 26.5 and 29.2 kcal mol^{-1} at the CCSD(T)//MP2 and G3//B3LYP theory levels, respectively. These values reduce to 21.0 and 23.8 kcal mol^{-1} for the fluorinated system and 21.8 and 23.5 kcal mol^{-1} for the chlorinated one.

The decomposition of halomethyl nitrates and halomethyl peroxynitrites to radical pair, $CHX_2ONO_2 \rightarrow CHX_2O + NO_2$ and $CHX_2OONO \rightarrow CHX_2O + NO_2$, takes place through the transition state configurations TS1*MP2* and TS2*MP*, respectively, that have been determined at the MP2 level (included also in Figures 1 and 2). These transition states are found to be loose geometries with relaxed CO—N and CO—O distances, located lower or at a comparable level in energy with CHX_2O + NO_2 and identified from one imaginary frequency as first-order saddle points at the MP2 level of theory. Thus, they do not represent real energy barriers, but they may rather be considered as wiggles on the PES, in agreement with the reported findings[30] about the barrierless dissociations of ROONO and $RONO_2$ to RO + NO_2. TS1*MP2* in particular bears many similarities with an analogous loose transition state structure calculated in the HOONO surface.[48]

The activated halomethyl nitrates may dissociate to the very stable carbonylated products, CHXO + XNO_2 and CX_2O + HONO through the transition states TS*cxho* and TS*cx₂o*, respectively. TS*cxho* presents a four-member ring geometry resulting from a considerable elongation of the two breaking

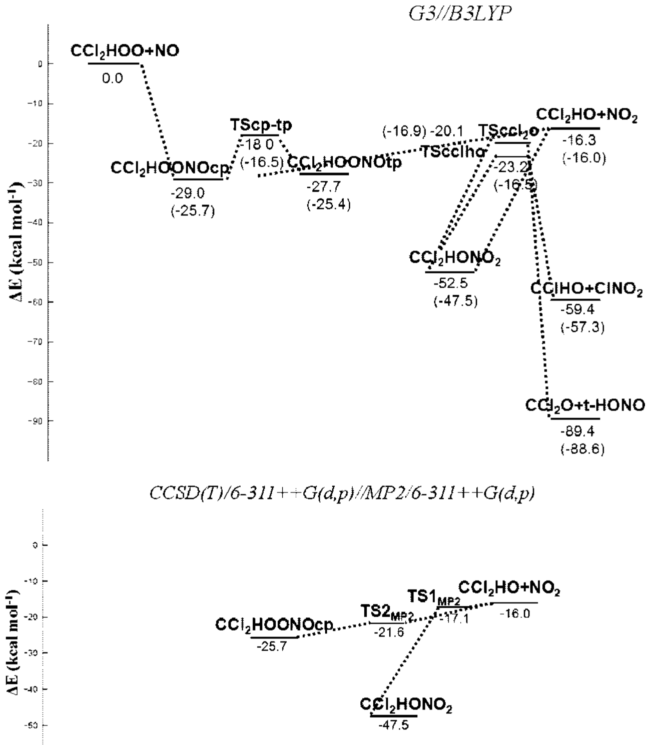

Figure 3. Energy profile for the reaction $CHCl_2O_2$ + NO. The numbers in parentheses are the CCSD(T)//B3LYP results. Only one line indicating the dissociation to $CHX_2O + NO_2$ from the CHX_2OONO conformers has been drawn to avoid overburden of the diagram.

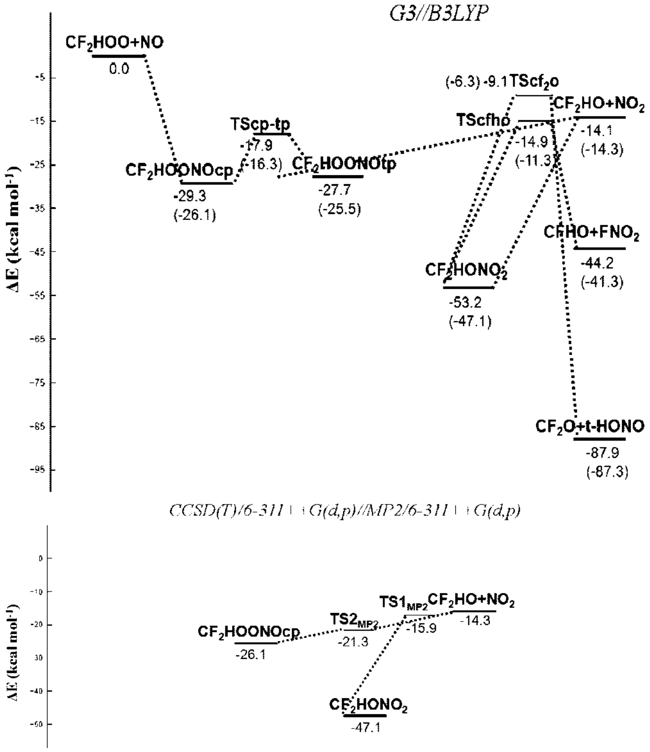

Figure 4. The same as in Figure 3 for the reaction CHF_2O_2 + NO.

C−F and N−O bonds and the attack of fluorine to the N atom. TS*cx₂o* displays a five-member cyclic structure formed through the approach of H to one of the terminal O atoms of the NO_2 fragment and the stretching of the inner CO−N bond. Comparison of the corresponding barriers with the methyl system (Table 2) shows a gradual reduction from X = H to X = Cl

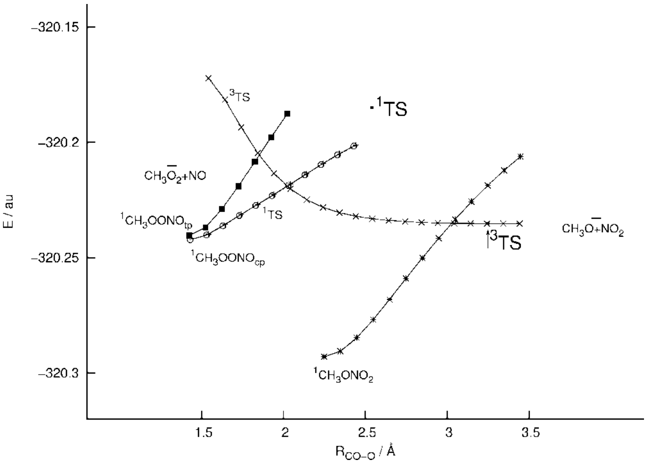

Figure 5. Potential energy curves for $^1CH_3OONO$, $^1CH_3ONO_2$, and ^{3}TS at the B3LYP level of theory as a function of the CO−O distance.

and an interesting difference between the fluorinated and chlorinated systems. In the chlorinated case, the critical energies involved for both carbonylated products formation are close to each other and both lower than the critical energy required for the radical pair decomposition pathway, $CHCl_2ONO_2 \rightarrow CHCl_2O + NO_2$. In the fluorinated system, however, TS*cf₂o* transition state is placed distinctly higher than either TS*cfho* or $CHF_2O + NO_2$, which are located at about the same energy level. Thus, dichloromethyl nitrate leads upon dissociation to both carbonylated products, whereas difluoromethyl nitrate most probably produces nitryl fluoride, that is, $CFHO + FNO_2$. The conclusion is in agreement with the experimental evidence about the decomposition of the related trifluorinated methyl nitrate. CF_3ONO_2 is a colorless gas with a boiling point of −18 ± 3 °C and a melting point of −163 °C which has been synthesized recently.[49,50] Experimentally, it was observed that trifluorinated methyl nitrate decays slowly into carbonyl fluoride, F_2CO, and nitryl fluoride, FNO_2, at room temperature in the gas phase and at lower temperatures in the liquid phase.

Peroxy Nitrite to Nitrate Isomerization, ROONO ↔ $RONO_2$. The results discussed previously reconfirm that the mechanism of the overall reaction $RO_2 + NO \rightarrow RO + NO_2$ is governed by the formation of the association intermediate, that is, the activated alkyl peroxynitrite in both conformeric forms and the exothermicity of the radical pair production pathway, $RO + NO_2$. No energy barriers have been encountered in any step of this process, and no alkyl nitrate formation pathway has been found to play any significant role in it, although trace amounts of alkyl nitrates have been repeatedly observed experimentally in the reactions of alkylperoxy radicals with NO. However, apart from the very low pressure region where alkyl nitrates might hypothetically assume a remote probability to be formed through the recombination reaction $RO + NO_2 \leftrightarrow RONO_2$, some one-step ROONO ↔ $RONO_2$ rearrangement process must operate in order to account for the alkyl nitrates formed under a more realistic range of pressures. No plausible one-step mechanism has been suggested yet. As already described in length in the Introduction, the reported $CH_3OONOtp \leftrightarrow CH_3ONO_2$ isomerization transition state for the maternal methyl system, denoted as TS*ono-no2*,[28] and determined at both the MP2 and B3LYP levels of theory by using a restricted wave function, was shown to be unstable with respect to the unrestricted wave function. When the transition state was treated by unrestricted methodology (UB3LYP) and with the use of broken-symmetry wave function (guess=mix) in the

TABLE 2: Relative Energies (kcal mol^{-1}) Including Zero-Point Energy Corrections of the Important Energy Minima and Transition States with Respect to CHX_2O_2 + NO (X = H[a], F, Cl, Br[b]), by Using the 6-311++G(d,p) Basis Set

species	MP2	B3LYP	CCSD(T)//MP2	CCSD(T)//B3LYP	G2MP2	G3//B3LYP
$CH_3OONOcp$	−30.4	−17.8	−21.0	−18.3	−26.3	−24.6
$CH_3OONOtp$	−28.9	−16.6	−19.6	−17.5	−24.9	−23.2
TS*cp-tp*	−20.1	−5.2	−10.0	−7.3	−13.5	−12.4
CH_3ONO_2	−64.8	−47.7	−47.5	−45.2	−54.9	−53.8
TS$\mathit{ch_2o}$	−24.0	−9.7	−4.0	−6.6	−12.1	−10.5
TS1*MP2*	−28.5		−9.2			
TS2*MP2*	−17.2		−12.3			
CH_3O+NO_2	−22.0	−15.7	−11.0	−11.7	−10.6	−12.4
$CH_2O+HONO$	−82.2	−65.2	−67.3	−70.0	−72.1	−70.4
$CHF_2OONOcp$	−36.0	−22.8	−26.1	−23.9	−30.4	−29.3
$CHF_2OONOtp$	−34.1	−21.5	−25.5	−22.7	−29.0	−27.7
TS*cp-tp*	−26.1	−11.4	−16.3	−13.6	−18.8	−17.9
CHF_2ONO_2	−64.8	−47.4	−47.1	−45.0	−52.4	−53.1
TS$\mathit{cf_2o}$	−24.7	−9.7	−6.3	−3.1	−9.6	−9.1
TS*cfho*	−38.7	−16.8	−11.3	−8.4	−14.5	−14.9
TS1*MP2*	−39.9		−15.9			
TS2*MP2*	−28.4		−21.3			
$CHF_2O + NO_2$	−24.2	−18.4	−14.3	−13.0	−12.1	−14.1
CF_2O + HONO	−100.7	−84.2	−87.3	−84.0	−88.8	−87.9
CHFO + FNO_2	−61.7	−45.1	−41.3	−38.8	−44.1	−44.2
$CHCl_2OONOcp$	−36.1	−21.6	−25.7	−22.8	−30.6	−29.0
$CHCl_2OONOtp$	−34.5	−20.7	−25.4	−21.9	−29.6	−27.7
TS*cp-tp*	−26.6	−10.7	−16.5	−12.8	−19.4	−18.0
$CHCl_2ONO_2$	−66.3	−47.6	−47.5	−44.0	−53.2	−52.5
TS$\mathit{ccl_2o}$	−37.1	−20.2	−16.5	−13.5	−22.2	−20.0
TS*cclho*	−43.3	−25.7	−16.8	−13.8	−23.1	−23.2
TS1*MP2*	−43.8		−17.1			
TS2*MP2*	−29.0		−21.6			
$CHCl_2O + NO_2$	−24.3	−22.7	−16.0	−13.5	−14.3	−16.3
CCl_2O + HONO	−101.3	−86.9	−88.6	−85.1	−91.0	−89.4
CHClO + $ClNO_2$	−74.5	−62.5	−57.3	−53.5	−60.9	−59.4
$CHBr_2OONO$			−27.5			
$CHBr_2O + NO_2$[b]			−17.4			

[a] Data taken from ref 28. [b] Data taken from ref 34 calculated at the CCSD(T)/cc-pVTZ//MP2/6-311+G(d,p) level.

optimization process, the geometry and energy remain unaltered. The calculated structure has been claimed to be an artifact of the calculation,[29] and higher multiconfigurational perturbation theory techniques[30] have shown that the computed configuration is in reality a S_1/S_0 conical intersection. Thus, the question about some plausible one-step isomerization mechanism that could describe the formation of methyl nitrate in the CH_3O_2 + NO and the general RO_2 + NO reactions remains unresolved. And once the unimolecular rearrangement issue finds a satisfactory interpretation for the plain methyl system, extrapolation and analogous deductions may then be adopted and worked out for the halogenated reactions.

By following this reasoning, we have devoted many efforts to the search of an acceptable pathway for the isomerization process, $CH_3OONO \leftrightarrow CH_3ONO_2$ with no successful results. Among the various approaches attempted in this tedious investigation, an assumption has been made to accept the potential role of biradicaloid nitrite states analogous to those discussed in the peroxynitrous acid case[51] in correlation with the involvement of the triplet surface. No such species have been investigated specifically in the present work, but similar biradicaloid methylperoxy nitrite singlet states could be possibly accessed by the activated methylperoxy nitrite singlet ground-state configuration, which then may easily correlate with the triplet PES. This thought has led to the search of a triplet isomerization transition state, ^{3}TS, in the place of the ambiguous ^{1}TS'TS*ono-no2* configuration (we keep referring to the unstable (U)B3LYP calculated TS*ono-no2* structure just for notation reasons). Indeed, a bound triplet transition-state structure has been found at the (U)B3LYP//6-311++G(d,p) level of theory, for which the stability check showed a stable wave function under the perturbations considered. The expectation value of the ⟨S2⟩ operator for ^{3}TS was not greater than 2.03. Both singlet and triplet transition-state structures were also reevaluated by using the (U)CCSD method based on the B3LYP optimized geometries. The T^1 diagnostic[52] in CCSD are 0.026 for the singlet and 0.023 for the triplet transition state, which are close to the 0.02 cutoff recommended for considering a problem to be single reference. The largest amplitudes of the single and double excitations in the CCSD wave function, another check of the accuracy of the single-determinant assumption, were 0.41 for the singlet and 0.06 for the triplet transition state.

Furthermore, in trying to elucidate a plausible potential energy path, we followed in Figure 5 both the singlet and the triplet potential energy curves for the one-step rearrangement pathway of cis or trans peroxy nitrite to nitrate. The calculations have been carried out at the B3LYP/6-311++G(d,p) level of theory, by increasing the CO—ONO bond distance in steps of 0.1 Å, starting from the optimized geometries of CH_3OONO, CH_3ONO_2, and ^{3}TS and performing full optimization of the remaining structural parameters. The triplet isomerization transition state presents a geometry quite similar to that of the unstable singlet one,[28] ^{1}TS≡TS*ono-n,o*$_2$, except for one main difference: the CO—ONO distance is elongated from 2.542 Å in ^{1}TS to 3.248 Å in ^{3}TS, which is essentially a weak interacting, almost dissociated species. It is also found considerably lower in energy, ~6.5 kcal mol^{-1} at the G3//B3LYP level. Several interesting correlations can be observed in these results. The most important is that the potential energy curve starting from $^1CH_3OONO$ optimized structure and which assumingly traces the ^{1}TS curve

TABLE 3: Heat of Formation Values,[a] ΔH_f^0 (kcal mol^{-1}), of the Important Energy Minima in the reactions CHX_2O_2 + NO (X = H[b], F, Cl)

species	CCSD(T)//MP2	CCSD(T)//B3LYP	G2MP2[d]	G3//B3LYP	CBS-QB3
$CH_3OONOcp$			−2.4	2.2	0.1
$CH_3OONOtp$			−0.9	3.7	1.5
CH_3ONO_2			−30.7	−26.9	−29.3
					−29.2 ± 1.1[c]
$CHF_2OONOcp$			−111.2	−103.8	−107.5
	−101.6	−101.5	−108.0	−105.3	
$CHF_2OONOtp$			−109.8	−102.1	−105.8
	−99.3	−100.9	−106.5	−103.2	
CHF_2ONO_2			−133.2	−127.6	−131.4
	−121.6	−122.5	−129.9	−129.1	
			−127.9		
$CHCl_2OONOcp$			−17.3	−9.4	−14.9
	−8.6	−9.2	−15.7	−12.0	
$CHCl_2OONOtp$			−16.3	−8.2	−13.5
	−7.8	−8.9	−14.6	−10.8	
$CHCl_2ONO_2$			−39.9	−32.9	−38.2
	−30.0	−31.0	−38.3	−35.6	
			−35.4		

[a] The first line of results for each halogenated species are based on the atomization energies,[45,46] the second line on eq 3b, and the third line on the isodesmic scheme of eq 4. [b] From refs 36 and 37. [c] This is the most recent ΔH_f^{298} value from ref 20.

as the CO—ONO increases becomes indeterminable in the range of interest of the CO—ONO values where the unstable ^{1}TS optimized structure was supposed to be located. This significant result agrees with the ambiguities expressed about the existence of this configuration. The ^{3}TS curve on the other hand presents a continuous smooth curve that crosses both the $^1CH_3OONO$ and the $^1CH_3ONO_2$ lines. On the basis of these findings, we might suggest that the unimolecular peroxynitrite to nitrate mechanism involves both the triplet and the singlet surfaces. $^1CH_3OONO$ may first convert to a biradicaloid species which crosses easily to the triplet ^{3}TS curve at ~2 Å and follows this curve instead of the discontinuous ^{1}TS curve. At ~3.1 Å, the system still being on the ^{3}TS curve encounters the second crossing with the $^1CH_3ONO_2$ line and isomerizes this way into methyl nitrate. It is worth mentioning that the structures of methyl peroxynitrite with elongated the O—O bond length around 3 Å almost involves the partial dissociation of CH_3OONO; thus, the curve in Figure 5 should approach the dissociation limit, that is, the CH_3O + ONO asymptote. But the energy curve increases with further elongation, which can be ascribed to a computational artifact of the B3LYP method.

The two-state diabatic model suggested above does seem reasonable in view of other radical−radical systems, where the involvement of the triplet surface in the reaction mechanism has been discussed, for instance the CH_3 + NO[53] and the BrO + NO_2[54] reactions. Davies et al.[53] in particular have calculated in detail the contribution of the triplet state, accepting its involvement as the most plausible way to rationalize the experimental kinetics of the association reaction between CH_3 and NO. The unimolecular rearrangement of trans-FONO to FNO_2 has also been described qualitatively in terms of a two-state diabatic model involving the F atom and the ground and first excited σ states of NO_2.[55] Certainly, further investigation and higher level calculations are required for the present system in order to establish the triplet isomerization transition state as the reliable pathway for the formation of methyl nitrate. However, the one-step mechanism proposed is reasonable and surely complies with one fact, namely, that the alkyl nitrate production most probably takes place in a unimolecular process[56] and that any two-step bimolecular recombination mechanism for its formation is less likely.

In summarizing the findings about the nitrate formation mechanism, we would like to emphasize the correlation between the stabilization trends calculated in the present work for the halogenated systems from one side and the nitrate yield on the other, via the adoption of the suggested one-step unimolecular rearrangement for nitrate formation. As described in detail, halogenated methyl peroxynitrites are found to present larger stabilization energies relative to RO_2 + NO compared to the plain methyl peroxynitrite. This interesting result ought to affect favorably the production yield of halomethyl nitrates through the one-step peroxynitrite ↔ nitrate isomerization mechanism suggested and, thus, allows to attribute the increased nitrate yield observed experimentally to the higher halomethyl peroxynitrite stabilization. Indeed, the recent experimental measurements by Nishida et al.[16] confirm these arguments. In addition to the determination of the rate constant of the reaction CF_3O_2 + NO, they have also measured the CF_3ONO_2 yield and compared it to that of CH_3ONO_2 from CH_3O_2 + NO.[21] At 700 Torr and 296 K, they found that the branching ratio is k(nitrate) / k(total) = $(1.67 \pm 0.27) \times 10^{-2}$. Thus, fluorination of the methyl group means that, at near room temperature and 1 atm pressure conditions, CF_3O_2 radicals produce at least three times more nitrate than CH_3O_2. The result directly associates with both the higher stabilization of the peroxynitrite species, CF_3OONO, and the nitrate formation mechanism suggested through the one-step isomerization $CF_3OONO \leftrightarrow CF_3ONO_2$ via an analogous two-state diabatic model for the CF_3O_2 + NO system.

Heat of Formation Results. Thermodynamic stability is a very crucial property to consider when discussing the role of the various volatile organic compounds in the atmosphere. Heat of formation values for the methyl peroxynitrite and nitrate derivatives investigated in the present work are calculated with the methods described in the Computational Details and are summarized in Table 3. In the calculations based on the ab initio dissociation energies of eq 3 and the isodesmic scheme of eq 4, the experimental heat of formation values for the CH_2X_2, CHX_2O, and NO_2 species have been used.[20,57,58] Comparison of the computed and experimental heat of formation of methyl nitrate, CH_3ONO_2, as tabulated in the most recent NASA-JPL tables, shows excellent agreement. Also good agreement is obtained among the results for the halogenated nitrates from all other methods.

There is no doubt that halogenation affects the thermodynamic stability of halomethyl peroxynitrites, CHX_2OONO relative to $CHX_2O_2 + NO$ and halomethyl nitrates, CHX_2ONO_2 relative to $CHX_2O + NO_2$, for X = F, Cl. A striking feature is the high thermodynamic stability of the fluorinated derivatives, which has been observed for other fluorinated species too and which reflects the particular strength of the C—F bond.

Summary

The effect of halogenation on the energetics of the reaction between the halomethylperoxy radicals, CHX_2O_2, and NO (X = F, Cl) has been examined by using ab initio and density functional theory quantum mechanical methods. The reaction mechanism involves the intermediate formation of the halomethyl peroxynitrite CHX_2OONO and its barrieless dissociation to radical pair $CHX_2O + NO_2$. The isomeric halomethyl nitrates that are the association intermediates in the reverse recombination reaction $CHX_2O + NO_2$ are found to dissociate to the carbonylated products $CHXO + XNO_2$, $CX_2O + HONO$, X = F, Cl.

Detailed comparison with literature data is carried out for the $CH_3O_2 + NO$ and $CHBr_2O_2 + NO$ reactions. The calculations confirm the increased attractive character of the PES upon halogenation and justify the higher overall rate coefficients and the larger halomethyl nitrate yields measured in the case of the halogenated systems. More specifically, the increased reactivity is attributed to the higher entrance well corresponding to the more stable halomethyl peroxy nitrite intermediates and the larger exothermicity of the overall $CHX_2O_2 + NO \rightarrow CHX_2O + NO_2$ reaction compared to $CH_3O_2 + NO \rightarrow CH_3O + NO_2$.

The isomerization pathway for the maternal system, $CH_3OONO \leftrightarrow CH_3ONO_2$, through which traces of methyl nitrates are formed in the reactions of methylperoxy radicals with NO, has been reexamined in view of the instability of the reported isomerization transition state $^1TS \equiv TS\textit{ono-no}_2$, calculated at the B3LYP and MP2 levels on the singlet surface.[28] A bound triplet isomerization transition state has been determined instead, which is found to be stable with respect to the wave function stability requirements. Accordingly, a two-state diabatic model is proposed to explain the nitrate formation which is suggested to take place through the crossings of the singlet $^1CH_3OONO$ and $^1CH_3ONO_2$ curves with the triplet ^3TS line.

Acknowledgment. The work was funded in part by the Ministry of Higher Education, Science and Technology of Slovenia, program grant number P2-0148 and in part by the General Secretariat for Research and Technology of Greece, program grant number 61/1864. We are grateful for their support.

Supporting Information Available: Optimized structures and harmonic vibrational frequencies for energy minima and transition states. This information is available free of charge via the Internet at http://pubs.acs.org.

References and Notes

(1) Finlayson-Pitts, B. J.; Pitts, J. N., Jr. *Chemistry of the Upper and Lower Atmosphere*; Academic Press: London, 2000.

(2) Wallington, T. J.; Nielsen, O. J.; Sehested, J. Reactions of Organic Peroxy Radicals in the Gas Phase. In *Peroxy Radicals*; Alfassi, Z., Ed; Wiley& Sons: New York, 1997.

(3) Arey, J.; Aschmann, S. M.; Kwok, E. S. C.; Atkinson, R. *J. Phys. Chem. A* **2001**, *105*, 1020.

(4) Shepson, P. B. Organic Nitrates. In *Volatile Organic Compounds in the Atmosphere*; Koppmann, R., Ed; Blackwell Publishing: Oxford, 2007, and references therein.

(5) Plumb, I. C.; Ryan, K. R. *Chem. Phys. Lett.* **1982**, *92*, 236.

(6) Caralp, F.; Lesclaux, R.; Dognon, A. M. *Chem. Phys. Lett.* **1986**, *129*, 433.

(7) Clemitshaw, K. C.; Sodeau, J. R. *J. Phys. Chem.* **1987**, *91*, 3650.

(8) Sehested, J.; Nielsen, O. J.; Wallington, T. J. *Chem. Phys. Lett.* **1993**, *213*, 457.

(9) Sehested, J.; Nielsen, O. J. *Chem. Phys. Lett.* **1993**, *206*, 369.

(10) Bevilacqua, T. J.; Hanson, D. R.; Howard, C. J. *J. Phys. Chem.* **1993**, *97*, 3750.

(11) Bhatnagar, A.; Carr, R. W. *Chem. Phys. Lett.* **1994**, *231*, 454.

(12) Turnipseed, A. A.; Barone, S. B.; Ravishankara, A. R. *J. Phys. Chem.* **1994**, *98*, 4594.

(13) Bourbon, C.; Brioukov, M.; Hanoune, B.; Sawerysyn, J. P.; Devolder, P. *Chem. Phys. Lett.* **1996**, *254*, 203.

(14) Wallington, T. J.; Bilde, M.; Møgelberg, T. E.; Sehested, J.; Nielsen, O. J. *J. Phys. Chem.* **1996**, *100*, 5751.

(15) Louis, F.; Burgess, D. R., Jr.; Rayez, M. T.; Sawerysyn, J. P. *Phys. Chem. Chem. Phys.* **1999**, *1*, 5087.

(16) Nishida, S.; Takahashi, K.; Matsumi, Y.; Chiappero, M.; Argüello, G.; Wallington, T. J.; Hurley, M. D.; Ball, J. C. *Chem. Phys. Lett.* **2004**, *388*, 242.

(17) Bayes, K. D.; Friedl, R. R.; Sander, S. P. *J. Phys. Chem. A* **2005**, *109*, 3045.

(18) Patchen, A. K.; Pennino, M. J.; Elrod, M. J. *J. Phys. Chem. A* **2005**, *109*, 5865.

(19) Hsin, H. Y.; Elrod, M. J. *J. Phys. Chem. A* **2007**, *111*, 613.

(20) Sander, S. P.; Friedl, R. R.; Golden, D. M.; Kurylo, M. J.; Moortgat, G. K.; Wine, P. H.; Ravishankara, A. R.; Kolb, C. E.; Molina, M. J.; Finlayson-Pitts, B. J.; Huie, R. E.; Orkin, V. L. Chemical Kinetics and Photochemical Data for Use in Atmospheric Studies: Evaluation Number 15. *JPL Publication 06-2*; National Aeronautics and Space Administration, Jet Propulsion Laboratory, California Insitute of Technology: Pasadena, CA, 2006.

(21) Eberhard, J.; Howard, C. J. *J. Phys. Chem. A* **1997**, *101*, 3360.

(22) Kirchner, F.; Zabel, F.; Becker, K. H. *Berichte Bun-Ges.* **1990**, *94*, 1379.

(23) King, M. D.; Thomson, K. C. *Atmos. Environ.* **2003**, *37*, 4517.

(24) Lohr, L. L.; Barker, J. R.; Stroll, R. M. *J. Phys. Chem. A* **2003**, *107*, 7429.

(25) Barker, J. R.; Lohr, L. L.; Stroll, R. M.; Reading, S. *J. Phys. Chem. A* **2003**, *107*, 7434.

(26) Zhang, J.; Dransfield, T.; Donahue, N. M. *J. Phys. Chem. A* **2004**, *108*, 9082.

(27) Zhao, Y.; Houk, K. N.; Olson, L. P. *J. Phys. Chem. A* **2004**, *108*, 5864.

(28) Lesar, A.; Hodošček, M.; Drougas, E.; Kosmas, A. M. *J. Phys. Chem. A* **2006**, *110*, 7898.

(29) Dibble, T. S. *Atmos. Environ.* **2008**, *37*, 4517.

(30) Arenas, J. F.; Avila, F. J.; Otero, J. C.; Peláez, Soto, J. *J. Phys. Chem. A,* **2008**, *112*, 249.

(31) Stimac, P. J.; Barker, J. R. *J. Phys. Chem. A* **2008**, *112*, 2553.

(32) Aschmann, S. M.; Long, W. D.; Atkinson, R. *J. Phys. Chem. A* **2006**, *110*, 6617.

(33) Cassanelli, P.; Fox, D. J.; Cox, R. A. *Phys. Chem. Chem. Phys.* **2007**, *9*, 4332.

(34) McGivern, W. S.; Francisco, J. F.; North, S. W. *J. Phys. Chem. A* **2002**, *106*, 6395.

(35) McGivern, W. S.; Kim, H.; Francisco, J. F.; North, S. W. *J. Phys. Chem. A* **2004**, *108*, 7247.

(36) Lesar, A.; Salta, Z.; Kovačič, S.; Kosmas, A. M. *Chem. Phys. Lett.* **2007**, *446*, 268.

(37) Kosmas, A. M.; Lesar, A. *Mol. Phys.* **2008**, *106*, 1025.

(38) Møller, C.; Plesset, M. S. *Phys. Rev.* **1934**, *46*, 618.

(39) Frisch, M. J.; Head-Gordon, M.; Pople, J. A. *Chem. Phys. Lett.* **1990**, *166*, 281.

(40) Becke, A. D. *J. Chem. Phys.* **1993**, *98*, 5648.

(41) Lee, C.; Yang, W.; Parr, R. G. *Phys. Rev.* **1988**, *37*, 785.

(42) Hehre, W. J.; Radom, L.; Schleyer, P. V. R.; Pople, A. J. *Ab initio Molecular Orbital Theory*; Wiley-Interscience: New York, 1986.

(43) Gonzales, C.; Schlegel, H. B. *J. Chem. Phys.* **1989**, *90*, 2154.

(44) Pople, J. A.; Gordon, M. H.; Ragavashari, K. *J. Chem. Phys.* **1987**, *87*, 5968.

(45) Montgomery, J. A., Jr.; Frisch, M. J.; Ochterski, J. W.; Petersson, G. A. *J. Chem. Phys.* **1999**, *110*, 2822.

(46) Curtiss, L. A.; Raghavachari, K.; Redfern, P. C.; Pople, J. A. *J. Chem. Phys.* **1997**, *106*, 1063.

(47) Frisch, M. J.; Trucks, G. W.; Schlegel, H. B.; Scuseria, G. E.; Robb, M. A.; Cheeseman, J. R.; Montgomery, J. A.; Jr., Vreven, T.;

Kudin, K. N.; Burant, J. C.; Millam, J. M.; Iyengar, S. S.; Tomasi, J.; Barone, V.; Mennucci, B.; Cossi, M.; Scalmani, G.; Rega, N.; Petersson, G. A.; Nakatsuji, H.; Hada, M.; Ehara, M.; Toyota, K.; Fukuda, R.; Hasegawa, J.; Ishida, M.; Nakajima, T.; Honda, Y.; Kitao, O.; Nakai, H.; Klene, M.; Li, X.; Knox, J. E.; Hratchian, H. P.; Cross, J. B.; Bakken, V.; Adamo, C.; Jaramillo, J.; Gomperts, R.; Stratmann, R. E.; Yazyev, O.; Austin, A. J.; Cammi, R.; Pomelli, C.; Ochterski, J.; Ayala, P. Y.; Cui, Q.; Morokuma, K.; Voth, G. A.; Salvador, P.; Dannenberg, J. J.; Zakrzewski, V. G.; Dapprich, S.; Daniels, A. D.; Strain, M. C.; Farkas, O.; Malick, D. K.; Rabuck, A. D.; Raghavachari, K.; Foresman, J. B.; Ortiz, J. V.; Cui, Q.; Baboul, A.; Clifford, S.; Cioslowski, J.; Stefanov, B. B.; Liu, G.; Liashenko, A.; Piskorz, P.; Komaromi, I.; Martin, R. L.; Fox, D. J.; Keith, T.; Al-Laham, M. A.; Peng, C. Y.; Nanayakkara, A.; Challacombe, M.; Gill, P. M. W.; Johnson, B.; Chen, W.; Wong, J. L.; Gonzalez, C.; Pople, J. A., Gaussian 03, Gaussian Inc., Wallingford, CT, 2004.

(48) Dixon, D. A.; Feller, D.; Zhan, C.-G.; Francisco, J. S. *J. Phys. Chem. A* **2002**, *106*, 3191.

(49) Sander, S.; Willner, H.; Oberhammer, H.; Argüell, G. A. *Z. Anorg. Allg. Chem.* **2001**, *627*, 655.

(50) Chiappero, M. S.; Burgos Paci, M. A.; Argüello, G. A.; Wallington, T. J. *Inorg. Chem.* **2004**, *43*, 2714.

(51) Bach, R. D.; Dmitrenko, O.; Estévez, C. M. *J. Am. Chem. Soc.* **2003**, *125*, 16204.

(52) Lee, T. J.; Taylor, P. R. *Int. J. Quant. Chem. Symp.* **1989**, *23*, 199.

(53) Davis, J. W.; Green, N. J. B.; Pilling, M. J. *J. Chem. Soc. Faraday Trans.* **1991**, *87*, 2317.

(54) Walsh, R.; Golden, D. M. *J. Phys. Chem. A* **2008**, *112*, 3891.

(55) Ellison, G. B.; Herbert, J. M.; McCoy, A. B.; Stanton, J. F.; Szalay, P. G. *J. Phys. Chem. A* **2004**, *108*, 7639.

(56) Ravelo, M. R.; Francisco, J. S. *J. Am. Chem. Soc.* **2008**, *130*, 11234.

(57) Zachariah, M. R.; Tsang, W.; Westmoreland, P. R.; Burgess, D. R. F., Jr. *J. Phys. Chem.* **1995**, *99*, 12512.

(58) Sun, H.; Bozzelli, J. W. *J. Phys. Chem. A* **2001**, *105*, 4504.

(59) Tyndall, G. S.; Cox, R. A.; Granier, C.; Lesclaux, R.; Moortgat, G. K.; Pilling, M. J.; Ravishankara, A. R.; Wallington, T. J. *J. Geophys. Res.* **2001**, *106*, 12157.

JP808895A